

EXPLORING THE LOCAL MILKY WAY: M DWARFS AS TRACERS OF GALACTIC POPULATIONS

JOHN J. BOCHANSKI¹, JEFFREY A. MUNN², SUZANNE L. HAWLEY¹, ANDREW A. WEST³, KEVIN R. COVEY⁴, DONALD P. SCHNEIDER⁵

Accepted to the Astronomical Journal

ABSTRACT

We have assembled a spectroscopic sample of low-mass dwarfs observed as part of the Sloan Digital Sky Survey along one Galactic sightline, designed to investigate the observable properties of the thin and thick disks. This sample of ~ 7400 K and M stars also has measured *ugriz* photometry, proper motions, and radial velocities. We have computed *UVW* space motion distributions, and investigate their structure with respect to vertical distance from the Galactic Plane. We place constraints on the velocity dispersions of the thin and thick disks, using two-component Gaussian fits. We also compare these kinematic distributions to a leading Galactic model. Finally, we investigate other possible observable differences between the thin and thick disks, such as color, active fraction and metallicity.

Subject headings: stars: low mass — stars: fundamental parameters — stars: M dwarfs — Galaxy: kinematics and dynamics — Galaxy: structure

1. INTRODUCTION

Modeling the Galaxy presents a challenging breadth of problems to both theorists and observers. Large N-Body simulations employing the constraints of gravity and Λ cold dark matter cosmology have sought to recreate the infant Galaxy, tracing the formation and collapse of baryons within the dark matter halo (Brook et al. 2004; Governato et al. 2007). Observationally, these simulations are constrained by rotational velocities and luminosity profiles of extragalactic systems (Dalcanton et al. 1997). Closer to home, observers seek to reconstruct the history of the Milky Way's cannibalistic mergers through photometric identification of tidal debris, such as the Sagittarius dwarf (Ibata et al. 1994). Spectroscopy is also employed to find surviving, co-moving stars of similar metallicity (e.g., Yanny et al. 2003).

A particularly interesting problem to both the theorist and observer is the formation and nature of the thick disk (Gilmore & Reid 1983). This population has been explored extensively, mainly through star counts (e.g. Gilmore & Reid 1983; Reid & Majewski 1993; Buser et al. 1999; Norris 1999; Siegel et al. 2002). However, the thick disk scale height and local density normalization are still uncertain (Norris 1999), with values of h_{thick} ranging from ~ 700 - 1500 pc and local normalizations between 2% and 15%. Larger scale heights are usually coupled to lower normalization values (see Figure 1 of Siegel et al. 2002). The scale length of the thick disk is also uncertain, though typically scale lengths larger than the thin disk are inferred (Chen et al. 2001; Larsen & Humphreys 2003). The thick disk is thought to be an older, metal-poor population (Reid & Majewski 1993;

Chiba & Beers 2000). Metallicity differences, such as α element enhancement, have been explored (Bensby et al. 2003), but other observables, such as photometric color and chromospheric activity trends, have yet to be studied in detail. Thick disks observed in external galaxies (Yoachim & Dalcanton 2006) often appear to have structural parameters and kinematics similar to the Milky Way.

Modeling the observable properties of the thin and thick disks, namely star counts (Reid & Majewski 1993; Reid 1993) and kinematics (Mendez & van Altena 1996; Robin et al. 2003; Vallenari et al. 2006), has undergone a resurgence in recent years. The seminal work of Bahcall & Soneira (1980) laid the foundation for modeling star counts of the smooth Galactic components. Present-day models, such as the Besançon model (Robin et al. 2003), and the Padova model (Vallenari et al. 2006) also incorporate kinematics, allowing for robust comparisons to observations. It is important to rigorously test their predictions against actual observed spatial and kinematic distributions.

Low-mass dwarfs are both ubiquitous and long-lived (Laughlin et al. 1997), and serve as excellent tracers of the Galactic potential (Wilson & Woolley 1970; Wielen 1977; West et al. 2006). Modern surveys, such as the Sloan Digital Sky Survey (SDSS; York et al. 2000), are sensitive to K and early M dwarfs at distances of ~ 1 kpc above the Galactic Plane, probing the transition between the thin (Reid et al. 1997) and thick (Kerber et al. 2001) disks. At these distances, we expect about 20% of the observed stars to be thick disk members, assuming a local normalization of 2% (Reid & Majewski 1993) and scale heights of 300 pc and 1400 pc for the thin and thick disks, respectively. Star counts of low-mass dwarfs have been used to determine Galactic structural properties (Reid et al. 1997 and references therein). These studies sought to determine the vertical scale height and local normalization of the thin and thick disks (Siegel et al. 2002), as well as the underlying mass function of these populations (Martini & Osmer 1998; Phleps et al. 2000; Covey et al. 2007a). The chemical evolution of the Galaxy has also been explored with red dwarfs (Reid et al. 1997), using

¹ Astronomy Department, University of Washington, Box 351580, Seattle, WA 98195
email: bochansk@astro.washington.edu

² US Naval Observatory, Flagstaff Station, 10391 W. Naval Observatory Road, Flagstaff, AZ 86001-8521

³ Astronomy Department, University of California, 601 Campbell Hall, Berkeley, CA 94720-3411

⁴ Harvard-Smithsonian Center for Astrophysics, 60 Garden Street, MS-72 Cambridge, MA 02138

⁵ Department of Astronomy and Astrophysics, The Pennsylvania State University, 525 Davey Lab, University Park, PA 16802

molecular band indices as a proxy for metallicity (Gizis 1997).

In addition to their utility as Galactic tracers, low-mass dwarfs have intrinsic properties, such as chromospheric activity (West et al. 2004; Bochanski et al. 2005; Schmidt et al. 2007), that can be placed in a Galactic context. Additionally, metallicity may be probed using subdwarfs (Lépine et al. 2003), readily identified by their spectra, which show enhanced calcium hydride (CaH) absorption. Subdwarfs have been easily detected in large-scale surveys such as the SDSS (West et al. 2004).

Kinematic studies of low-mass stars have a rich historical background. Samples are typically drawn from proper motion surveys, such as the New Luyten Two Tenths (NLTT) catalog (Luyten 1979) and the Lowell Proper Motion Survey (Giclas et al. 1971). Efforts have been made to identify nearby stars in these surveys, for example by Gliese & Jahreiss (1991). However, proper motion surveys possess inherent kinematic bias. The McCormick sample (Vyssotsky 1956), assembled from 875 spectroscopically confirmed K and M dwarfs, has been frequently studied as a kinematically unbiased sample (Wielen 1977; Weis & Uppgren 1995; Ratnatunga & Uppgren 1997), although it has been suggested that the sample may be biased towards higher space motions (Reid et al. 1995). The Palomar-Michigan State University survey (PMSU; Reid et al. 1995; Hawley et al. 1996; Gizis et al. 2002; Reid et al. 2002) is among the largest prior spectroscopic surveys of low-mass stars, obtaining spectral types and radial velocities of ~ 1700 M dwarfs. The PMSU sample, which targeted objects from the Third Catalogue of Nearby Stars (Gliese & Jahreiss 1991), was used to construct a volume complete, kinematically unbiased catalog of ~ 500 stars, sampling distances to ~ 25 pc. Other surveys, such as the 100 pc survey (Bochanski et al. 2005), have also used low-mass stars as kinematic probes. In Table 1, we summarize the sample sizes and approximate distance limits of previous major kinematic surveys of low-mass dwarfs, along with the mean velocity dispersions for each study. It is clear that our sample of several thousand stars out to distances of ~ 1 kpc results in a study of Galactic kinematics using low-mass stars with unprecedented statistical significance.

In this paper, we present our examination of the properties of the thin and thick disks using a SDSS Low-Mass Spectroscopic Sample (SLoMaSS) of K and M dwarfs that is an order of magnitude larger than previous samples. In §2, we describe the SDSS spectroscopic and photometric observations that comprise SLoMaSS. The resulting distances and stellar velocities are presented in §3. In §4, we detail our efforts to separate the observed stars into two populations, search for kinematic, metallicity and color gradients and compare our results to a contemporary Galactic model. Finally, §5 summarizes our findings.

2. OBSERVATIONS

2.1. SDSS Photometry

The SDSS (York et al. 2000; Stoughton et al. 2002; Pier et al. 2003; Ivezić et al. 2004) is a large ($\sim 10,000$ sq. deg.), multi-color (*ugriz*; Fukugita et al. 1996; Gunn et al. 1998; Hogg et al. 2001; Smith et al. 2002; Tucker et al. 2006) photometric and spectroscopic survey centered on the Northern Galactic Cap. The 2.5m telescope

(Gunn et al. 2006), located at Apache Point Observatory scans the sky on great circles, as the camera (Gunn et al. 1998) simultaneously images the sky in five bands to a faint limit of ~ 22.2 in *r*, with a typical uncertainty of $\sim 2\%$ at $r \sim 20$ (Ivezić et al. 2003; Adelman-McCarthy et al. 2006). The last data release (DR5⁶; Adelman-McCarthy et al. 2007) comprises 8000 sq. deg. of imaging, yielding photometry of ~ 217 million unique objects, including ~ 85 million stars. SDSS photometry has enabled a myriad of studies on both Galactic structure (e.g. Yanny et al. 2000; Newberg et al. 2002; Juric et al. 2005; Belokurov et al. 2006) and low-mass stars (e.g. Hawley et al. 2002; Walkowicz et al. 2004; West et al. 2005; Davenport et al. 2006).

2.2. SDSS Spectroscopy

When sky conditions prohibit photometric observations, the SDSS telescope is fitted with twin fiber-fed spectrographs. These instruments simultaneously obtain 640 medium-resolution ($R \sim 1,800$), flux-calibrated, optical (3800–9200 Å) spectra per 3° plate, permitting radial velocity measurements for most stars with an uncertainty of ~ 10 km s⁻¹ (Abazajian et al. 2004). A typical 45 minute observation yields a signal-to-noise ratio per pixel > 4 at $g = 20.2$ and $i = 19.9$ (Stoughton et al. 2002), with a broadband flux calibration uncertainty of $\sim 4\%$ (Abazajian et al. 2004). The DR5 sample includes over 1 million spectra, with $\sim 216,000$ stellar spectra (Adelman-McCarthy et al. 2007). The majority of spectra in the SDSS database are drawn from 3 main samples, which target objects based on their photometric colors and morphological properties. These samples are optimized to observe galaxies (Strauss et al. 2002), luminous red galaxies with $z \sim 0.5 - 1.0$ (Eisenstein et al. 2001), and high redshift quasars (Richards et al. 2002). However, low-mass stars have similar colors to some of these samples and therefore are observed serendipitously. SDSS spectroscopy of late-type dwarfs has been the focus of numerous studies (see Hawley et al. 2002; Raymond et al. 2003; West et al. 2004; Silvestri et al. 2006; West et al. 2006; Bochanski et al. 2007 and references therein).

2.3. SDSS Low-Mass Spectroscopic Sample: SLoMaSS

During Fall 2001, a call was placed to the SDSS collaboration to design special spectroscopic plates that employed different targeting algorithms than the usual SDSS survey samples described in §2.2. We designed and proposed a series of observations to probe the local vertical structure of the Milky Way, obtaining spectra of low-mass dwarfs in the southern equatorial stripe (stripe 82) of the SDSS photometric footprint during Fall 2002. This stripe at zero declination is repeatedly observed during the time of the year when the Northern Galactic Cap is not visible. These repeat scans sample an area of ~ 300 sq. deg. and have been used to study Type Ia supernovae (Sako et al. 2005; Frieman et al. 2007), stellar variability (Sesar et al. 2007) and characterize the repeatability of SDSS photometry (Ivezić et al. 2007). SLoMaSS is comprised of stars with unsaturated *griz* photometry and extinction-corrected magnitude limits of $15 < i < 18$ and $i - z > 0.2$. A series of three spectroscopic tilings

⁶ <http://www.sdss.org/dr5/>

TABLE 1
 PREVIOUS LOW-MASS STELLAR KINEMATIC SURVEY RESULTS

| Study | Sample Size | Distance Limit (pc) | σ_U ^a | σ_V | σ_W | Comments |
|--------------------------------------|-------------|---------------------|-------------------------|------------|--------------------|--------------------------------------|
| Vyssotsky (1956); Reid et al. (1995) | 368 | ~ 300 | 39 | 26 | 23 | McCormick stars in PMSU survey |
| Wielen (1977) | 516 | ~ 300 | 39 | 23 | 20 | McCormick stars |
| Reid et al. (1995) | 514 | 25 | 43 | 31 | 25 | PMSU I volume-complete sample |
| Ratnatunga & Upgren (1997) | 773 | ~ 300 | 30.6 | 18.5 | 7.4 | McCormick stars |
| Reid et al. (2002) | 436 | 25 | 37.9 | 26.1 | 20.5 | PMSU IV volume-complete sample |
| | | 25 | 34 | 18 | 16 | PMSU IV volume-complete sample, core |
| Bochanski et al. (2005) | 419 | 100 | 35 | 21 | 22 | Non-active stars, core |
| | 155 | 100 | 19 | 15 | 16 | Active stars, core |
| This study | 70 | 100 | 28.4 | 21.3 | 19.2 | $ z < 100$ pc |
| | | 100 | 25.7 | 20.9 | 14.1 | $ z < 100$ pc, core |
| | 4300 | 500 | 39.0 | 30.0 | 24.8 | $ z < 500$ pc |
| | | 500 | 34.1 | 24.6 | 20.9 | $ z < 500$ pc, core |
| | 6893 | 1000 | 44.1 | 36.9 | 27.9 | $ z < 1000$ pc |
| | | 1000 | 37.4 | 27.2 | 23.6 | $ z < 1000$ pc, core |
| | 7398 | 1600 | 46.6 | 42.2 | 29.3 | Total Sample |
| | 1600 | 38.5 | 28.6 | 24.4 | Total Sample, core | |

^aThe velocity dispersions in U, V , and W are measured in km s^{-1} .

composed of 15 plates (numbers 1118-1132, centered on $l \sim 105^\circ$, $b \sim -62^\circ$) was observed, yielding a total of 8880 stellar spectroscopic targets in SLoMaSS, each with $ugriz$ photometry.

3. ANALYSIS

3.1. Spectral Types

The spectroscopic data were analyzed with the HAMMER suite of software (Covey et al. 2007b) which measures spectral type, $H\alpha$ emission line properties, and various spectral band indices. This pipeline automatically assigns a spectral type to each star, then allows the user to confirm and adjust the spectral type manually, if necessary. The accuracy of the final spectral types is ± 1 subtype. After examining the entire sample by eye, we selected spectroscopically confirmed K and M dwarfs. This cut decreased the sample from 8880 to 8696 stars. The final spectral type distribution of SLoMaSS, after the additional cuts explained below, together with the average $i - z$ color for each spectral type bin, is shown in Figure 1.

3.2. Distances - Photometric Parallax

Distances to the SLoMaSS stars were determined using the photometric parallax relations described in West et al. (2005) and Davenport et al. (2006). The West et al. (2005) relation was employed for stars with $i - z$ redder than 0.37 and the Davenport et al. (2006) parallax relation was applied to the bluer stars in SLoMaSS. We neglect reddening corrections, since the average extinction computed for the total column along this line of sight from Schlegel et al. (1998) was small (< 0.05 in i), and most of these stars will lie in front of significant amounts of dust. Stars with $i - z$ colors that did not fall within the appropriate boundaries of the photometric parallax relations ($0.22 < i - z < 1.84$) were removed from the sample, decreasing its size to 8280 stars. Additionally, we applied the photometric white dwarf-M dwarf pair cuts of Smolčić et al. (2004), removing 4 more stars from the

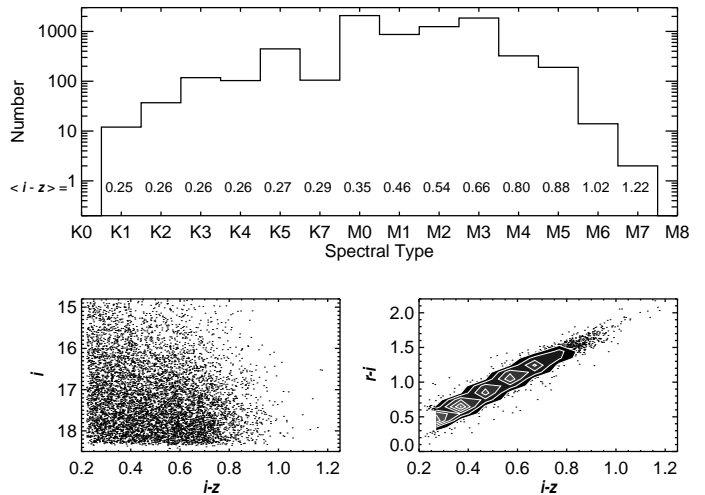


FIG. 1.— Upper panel: Distribution of spectral types within SLoMaSS. The mean $i - z$ color at each spectral type is shown above each bin. Lower panels: i vs. $i - z$ color-magnitude distribution and $r - i$ vs. $i - z$ color-color diagram of stars in SLoMaSS. The lowest contour (black) in the color-color diagram indicates a density of 100 stars in a square 0.1 magnitudes wide. Each additional contour represents 100 additional stars.

sample. The $i, i - z$ Hess diagram and $r - i, i - z$ color-color diagram are shown in the lower panels of Figure 1. The distance to the Galactic Plane was computed assuming the Sun's vertical position to be 15 pc above the Plane (Cohen 1995; Ng et al. 1997; Binney et al. 1997). The vertical distribution of stars in SLoMaSS is shown in Figure 2. Note that the decline in stellar density at large distances reflects the incompleteness of our sample, not the intrinsic stellar density, while the decline at small distances from the Plane is due to the saturation of SDSS

photometry.

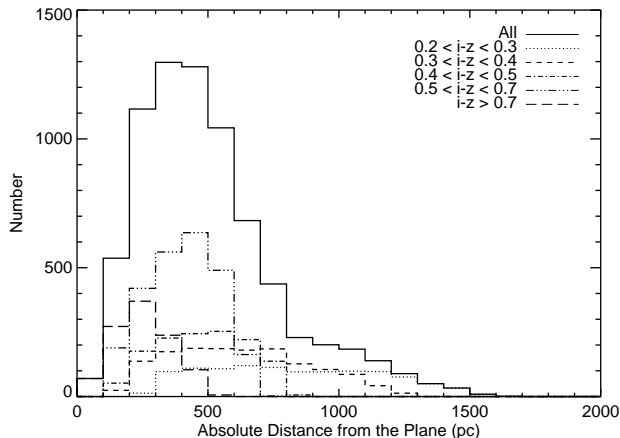


FIG. 2.— The absolute vertical distance distribution of the sample binned every 100 pc. The solid thick histogram is the total distribution, while the five remaining histograms represent the height distribution for five $i-z$ color bins as described in the legend. Note that there are hundreds of stars per bin out to an absolute vertical distance of ~ 1000 pc.

3.3. Distances - Spectroscopic Parallax

In addition to the photometric parallax relations mentioned above, we also computed the distances to the M dwarfs in SLoMaSS using the spectroscopic parallax relations of Hawley et al. (2002). These distances served as a check on the photometric parallax relations and were later used to divide the sample in a search for color differences between the thin and thick disks (see §4.3.2 for details). The spectroscopic parallax of K stars was not computed, as no reliable calibrated relations were available.

3.4. Radial Velocities, Proper Motions & UVW Velocities

Radial velocities were computed by cross-correlating the M dwarf stellar spectra against the low-mass template spectra of Bochanski et al. (2007) with the IRAF⁷ task *fxcor*. This cross-correlation routine is based on the method described in Tonry & Davis (1979). The measured velocities have external errors of ~ 4 km s⁻¹. The K dwarf radial velocities were obtained directly from the SDSS/Princeton 1D spectral pipeline⁸, with typical uncertainties of 10 km s⁻¹.

Proper motions were determined from the SDSS+USNO-B proper motion catalog (Munn et al. 2004). The catalog is $\sim 90\%$ complete over the magnitude limits of our sample, with random errors of ~ 3.5 mas yr⁻¹. We removed an additional 878 stars with poorly measured proper motions⁹, reducing our final sample size to 7398 stars.

⁷ IRAF is distributed by the National Optical Astronomy Observatories, which are operated by the Association of Universities for Research in Astronomy, Inc., under cooperative agreement with the National Science Foundation.

⁸ <http://spectro.princeton.edu>

⁹ Specifically, we required a match between catalogs (`match > 0`), detections in at least 4 plates in USNO-B (`nfit ≥ 5`), no other objects within 7 arcseconds, which is the resolution of the POSS plates (`dist22 > 7`; see Kilic et al. 2006), and small errors in the proper motion determination (`sigRA < 1000` and `sigDec < 1000`); see (Munn et al. 2004) for details.

Combining distances, proper motions and radial velocities, we computed the UVW space motions of each star in SLoMaSS using the method of Johnson & Soderblom (1987). The velocities are computed in a right-handed coordinate system, with positive U velocity directed toward the Galactic center and corrected for the solar motion (10, 5, 7 km s⁻¹; Dehnen & Binney 1998) with respect to the local standard of rest.

4. RESULTS

The SLoMaSS observations were used to investigate kinematics, colors, chromospheric activity and metallicity in the thin and thick disk populations.

We used two methods in our analysis. First, we examined the velocity distributions with no assumptions regarding the parent population of a given star (see §4.1). These kinematic results were then used to test a leading Galactic model (§4.2). We also used the space motion of each star to assign it to the thin or thick disk population, and investigated the color, metallicity and activity differences between the two populations (§4.3).

4.1. Kinematics

The sample was binned in 100 pc increments of vertical distance from the Galactic Plane and probability plots of UVW velocities were constructed (Lutz & Uppgren 1980; Reid et al. 1995, 2002). These diagrams plot the cumulative probability distribution in units of the standard deviation of the distribution. Hence, a single Gaussian distribution will appear as a straight line with a slope corresponding to the standard deviation of the sample and the y-intercept equal to the median of the distribution. Non-Gaussian distributions will significantly deviate from a straight line. An example of velocity distributions and their probability plots are shown in Figure 3. An advantage to this method is its immunity to outliers and to binning effects from poorly populated histograms.

For each distance bin in SLoMaSS, the probability plots are well fit with two lines: a low-dispersion, kinematically colder “core” component ($< |1\sigma|$) and a high-dispersion, “wing” component ($> |1\sigma|$). Shown in Figure 4 is an example of our analysis, illustrating linear fits to the core and wing distributions. At larger Galactic heights, the wing component traces the *in situ* thick disk population.

The resulting dispersions are shown as a function of distance from the Galactic Plane in Figure 5. The low-dispersion core component is well-behaved, smoothly increasing with increasing height. The high-dispersion wing component is subject to larger scatter, but generally increases with height from the Galactic Plane. Our results are summarized in Table 1. In order to facilitate comparison to the previous results included in the Table, we report the dispersions for several distance bins, as well as the entire sample.

4.2. Galactic Dynamical Models

4.2.1. Besançon Model: Introduction

Our sample is well suited to rigorously test current Galactic models. We chose the Besançon model (Robin et al. 2003) as a fiducial, since it simulates both star counts and kinematics. This model is constructed on several assumptions and empirical constraints, with the

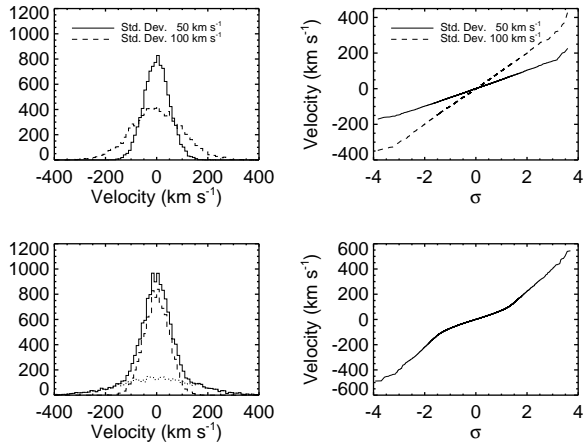


FIG. 3.— Schematics of velocity distributions (left panels) and their corresponding probability plots (right panels). The upper row displays two Gaussian distributions, one with a standard deviation of $\sim 50 \text{ km s}^{-1}$ (solid line) and another with a standard deviation of $\sim 100 \text{ km s}^{-1}$ (dashed line). A straight line in the probability plot signifies an underlying Gaussian distribution and the slope of the line is a measure of the standard deviation of the distribution. Note that the slope of the dashed line is twice that of the solid line. In the bottom row, a low dispersion component (dashed line) and high dispersion component (dotted line) are summed to produce the solid histogram. While the dual nature of the distribution is not readily apparent in the solid histogram, it is easily detected in the probability plot.

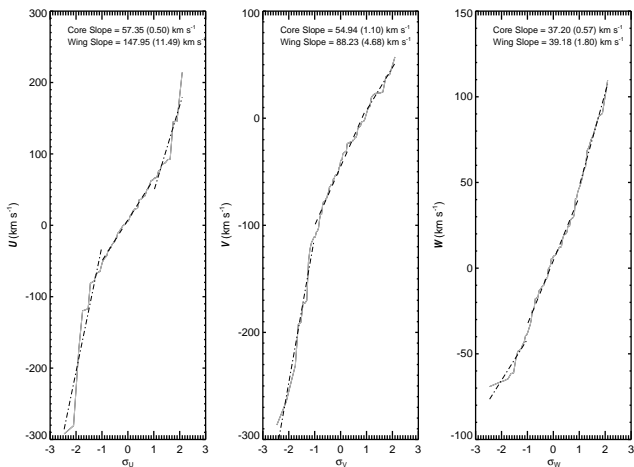


FIG. 4.— Illustrative example of our velocity dispersion analysis. Shown are probability plots for U , V and W for the $1200 < z < 1300$ pc bin (shaded lines). The “core” component (dashed line) is fit between $\pm 1 \sigma$, while the “wing” component (dot-dashed line) fits the outer edges of the distribution. Note the strong asymmetric drift component manifested as a change in slope at negative V velocities.

goal of reproducing the stellar content of the Milky Way. Four populations comprise the model: the thin and thick disks, bulge and halo. For each population, a star-formation history, initial mass function, density law and age are imposed. Additionally, an age-metallicity relation is employed for each population, with a Gaussian dispersion about the mean metallicity of each component (see Tables 1 and 3 of Robin et al. 2003).

Kinematically, the thin disk is composed of 7 groups of different ages (from 0.0 to 10 Gyr), each being isothermal except for the youngest (0.0 - 0.15 Gyr). The thick disk is composed of an 11 Gyr old population, with a ve-

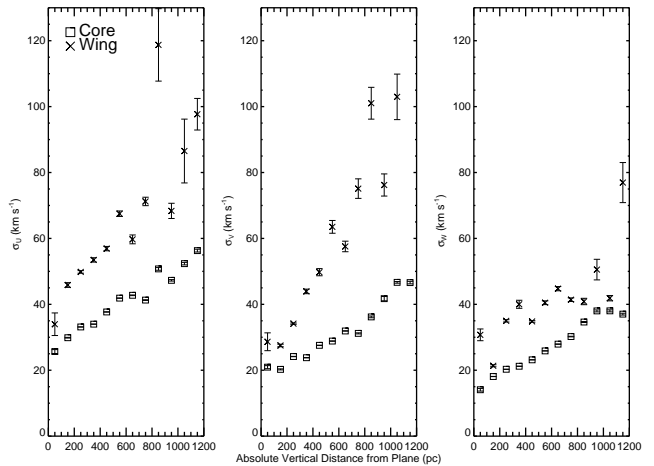


FIG. 5.— Velocity Dispersion as a function of vertical distance from the plane in 100 pc bins. The open squares represent the kinematically colder, core component and the crosses represent the high-dispersion, wing component. Errors are derived from the linear fits to the probability plots. Note the smooth trend in the low-dispersion component as a function of height from the Plane.

locity ellipsoid based on the measurements of Ojha et al. (1996, 1999). An age-velocity dispersion relation from Gomez et al. (1997) is imposed on each component, and the model is then allowed to self-consistently evolve to the present-day. This self-consistency is achieved with the method described in Bienayme et al. (1987). Stellar populations are formed according to their appropriate density laws and introduced with an initial velocity dispersion. The mass density of the stars is summed in a column of unit volume centered on the Sun along with dark matter halo and interstellar material contributions, and the potential is computed using the Poisson equation. Stars are then evolved using the collisionless Boltzmann equation in this new potential, and redistributed in the z direction, as complete orbital evolution is not included in this model. The process is iterated until the potential and scale heights of the disk populations converge at the 1% level. The local-mass density, which was empirically determined by Creze et al. (1998), also imposes a constraint on the initial Galactic potential. We note that imposing an age-velocity dispersion relation on the model dominates the kinematics, and that there are significant uncertainties in these relations. For example, the age-velocity dispersions used by Rocha-Pinto et al. (2004) differ by factors of ~ 2 for the oldest stars, compared to the relations in Gomez et al. (1997). These discrepancies are primarily derived from the difficulty in determining ages of field stars, with systematic differences imposed by various methods (i.e. isochrone fitting vs. chromospheric ages).

Intrinsic properties such as age, mass, luminosity, metallicity, position and velocity are available for each star in the simulation. Observable properties, such as colors, proper motions and radial velocities are also reported. To determine colors, the model uses the Lejeune et al. (1998) database, which employs adjusted stellar synthetic spectra that attempt to match empirical color-temperature relations.

4.2.2. Comparison to SDSS

We queried the Besançon webpage¹⁰, generating a suite of synthetic datasets along the appropriate Galactic sightline of SLoMaSS ($l \sim 105^\circ$, $b \sim -62^\circ$) with proper magnitude limits and error characteristics. We included both the thin and thick disks in the model inputs. The bulge and halo components were excluded since SLoMaSS points away from the bulge, and with a maximum distance of ~ 2000 pc, we expect halo contamination to be minimal. A total of 25 models were generated from identical input, in order to minimize Poisson noise.

As a consistency test of the Besançon model, we compared the model star counts to those obtained with SDSS survey photometry in the SLoMaSS field. We queried the SDSS Catalog Archive Server¹¹ for good point spread photometry¹² of stars along the appropriate sightline. This query resulted in 46,730 stellar targets. In the models, the mean star count was 46,991 with a standard deviation of 137. This excellent agreement should be viewed cautiously, as only rough magnitude cuts were imposed on the Besançon models, and we did not attempt to model observational problems that would affect SDSS star counts (Vanden Berk et al. 2005), such as cosmic rays or diffraction spikes near bright stars. However, the test inspires confidence that the Besançon model adequately represents the observed SDSS star counts.

4.2.3. Comparison to SLoMaSS

Each of the 25 models was sub-sampled to reproduce the color and distance distributions observed in SLoMaSS. The two-dimensional color-distance distribution was computed for SLoMaSS, and color-distance pairs were randomly drawn according to this normalized density distribution. If the color-distance pair was found in the Besançon model, then it was kept. This Monte-Carlo sampling continued until there were 7398 color-distance pairs, matching the number of stars in SLoMaSS. This sampling forced each model to simulate the properties of the SLoMaSS observations when compared to the complete SDSS photometry. Since SDSS $r - i$ colors are not available for the Besançon model, the SLoMaSS colors were transformed to $R - I$ using the relations of Davenport et al. (2006). Shown in Figure 6 are the $R - I$ and distance distributions for one instance of the model, along with those from SLoMaSS. Thus, each model is “observed” in a manner consistent with the spectroscopic observations of the SDSS field photometry.

4.2.4. Kinematic Comparisons

Using the sub-sampled model data, we compared the kinematic predictions of the Besançon models to the UVW velocities of SLoMaSS. Using the method described in §4.1, we constructed two sets of probability plots for each model: one composed of the thin and thick disk stars and one measured solely for the thin disk. The reason for this separation was twofold. The first was to isolate any systematics between the models thin and

thick disk predictions. Additionally, this allowed for direct testing comparison of the thin disk predictions, since most of these stars lie on the inner “core” region of the probability plot. That is, if the velocity predictions are correct for the thin disk, the overall slope of the isolated thin disk models should roughly match the “core” slope measured from SLoMaSS.

In Figure 7, an illustrative example of this analysis is shown. The main effect of adding the thick disk component is to increase the slope of both the core and wing components. Additionally, the wing component is enhanced, as seen in the W velocity distribution, which is expected from addition of a high dispersion population. It is clear from comparing to Figure 4 that the combination of the thin and thick disk model predictions are necessary to simulate the structure seen in the SLoMaSS data.

Following the method explained in §4.1 we measured the slopes of the “core” and “wing” components of the each model as a function of distance from the Galactic Plane. The results of this analysis, compared to the SLoMaSS results are shown in Figures 8 and 9. The SLoMaSS results (open squares), which are shown in Figure 5, are compared to the average Besançon prediction (crosses) for the thin (upper panels) and thick disk (lower panels). While the model does well in predicting general trends, there are clearly some systematics. The model predictions for the σ_W thin disk velocity dispersions are systematically low, suggesting there may be flaws in the method used to compute these motions. Additionally, the model underestimates the thick disk σ_V dispersions at large Galactic heights. As described above (§4.2), the assumed age-velocity dispersions relations, which dominate the predicted kinematic structure, are uncertain and may contribute to this disagreement. This speculation is supported by the results summarized in Table 1, which demonstrate that most previous surveys (as well as our own) have measured velocity dispersions significantly higher than those predicted from the model. The mean velocity distributions for both SLoMaSS and the Besançon model are shown in Figure 9. Again, the model in general performs well, but there are evident systematic differences. The mean V velocities predicted for the thin disk by the model are systematically high, and the thick disk V velocities diverge at large Galactic heights. The first difference may be attributed to our chosen solar motion values (10, 5, 7 km s⁻¹; Dehnen & Binney 1998). A larger adopted value of V_\odot , such as the classic value of 12 km s⁻¹ (Delhaye 1965), would move the mean velocities towards agreement. The discrepancy in the thick disk V velocities is probably due to small number statistics, as seen in Figure 2.

4.3. Differences between the Thin and Thick Disks

In order to examine observable differences between M dwarf members of the thin and thick disks, we kinematically separated the sample using the method of Bensby et al. (2003). This technique selects outliers in the wings of the three-dimensional Gaussian velocity distribution, and computes the probability of these stars belonging to the thick disk. The thin and thick disk populations were characterized by the velocity dispersions in Bensby et al. (2003). In order to minimize systematics, the UVW velocities were re-computed using distances determined

¹⁰ <http://physique.obs-besancon.fr/modele/>

¹¹ <http://cas.sdss.org/dr5/en/>

¹² Specifically, we required the following flags: a detection in BINNED1 and no EDGE, NOPROFILE, PEAKCENTER, NOTCHECKED, PSF_FLUX_INTERP, SATURATED, BAD_COUNTS_ERROR, DEBLEND_NOPEAK, CHILD, BLENDED, INTERP_CENTER or COSMIC_RAY flags set (Stoughton et al. 2002).

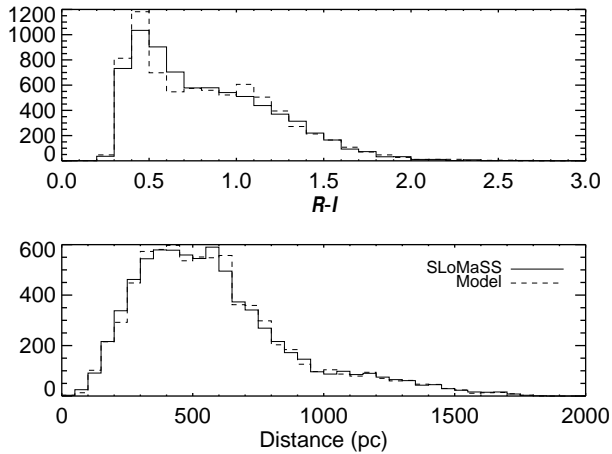


FIG. 6.— Shown are the $R - I$ and distance distributions of the stars in SLoMaSS (solid line) and a sampled model (dashed line). Note the agreement between the two datasets, indicating that we are sampling each instance of the Besançon model in a manner consistent with the spectroscopic observations in SLoMaSS.

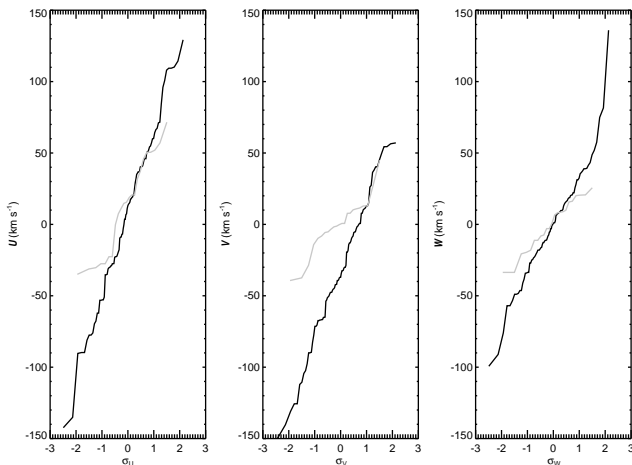


FIG. 7.— Probability Plots of the U , V and W velocities for pure thin disk (shaded line) and thin + thick models (solid line) in the $1200 < z < 1300$ pc bin. This height bin corresponds to the SLoMaSS data shown in Figure 4. Note that when the thick disk is added to the distribution, the overall slope increases, and the wing components are enhanced, as seen in the W probability plot. The combined thin and thick disk velocity distributions are also necessary to match the two-component structure seen in the SLoMaSS probability plots.

with the spectroscopic parallax relations of Hawley et al. (2002), as described above in §3.3. Thus, UVW should not *a priori* vary systematically with color. This also limits the analysis to the 6577 M dwarfs in the sample.

4.3.1. Metallicity

The exact formation mechanism of the thick disk is uncertain (see Majewski 1993 and references therein), but there is evidence that the mean metallicity of the thick disk is lower than that of the thin disk (Reid & Majewski 1993; Chiba & Beers 2000; Bensby et al. 2003). Additionally, differences in the α -element distributions have been shown to be distinct (Fuhrmann 1998; Feltzing et al. 2003; Bensby et al. 2003). While direct metallicity determinations of M dwarfs are difficult (Woolf & Wallerstein 2006), proxies of metallicity have been employed (Gizis 1997; Lépine et al. 2003; Bur-

gasser & Kirkpatrick 2006). These previous studies have used the low-resolution molecular band indices (CaH1, CaH2, CaH3, and TiO5) defined in Reid et al. (1995) to roughly discriminate between solar-metallicity, subdwarf ($[m/H] \sim -1.2$) and extreme-subdwarf ($[m/H] \sim -2$) populations. Adapting the methods of Lépine et al. (2003) and Burgasser & Kirkpatrick (2006) we computed the ratio $(\text{CaH2} + \text{CaH3}) / \text{TiO5}$ for each star in the sample, which varies such that a larger value indicates a higher metallicity. The mean ratio for each spectral type for the thin and thick disk populations is shown in Figure 10. The two populations do not separate within the errors, suggesting that the observed metallicity distributions do not differ greatly.

4.3.2. Color Gradients

A lower mean metallicity could also manifest itself as a color shift at a given spectral type. Specifically, West et al. (2004) showed that at a given $r - i$ or $i - z$ color, low metallicity subdwarfs ($[m/H] \sim -1.2$) were redder in $g - r$. After SLoMaSS was kinematically separated, the mean $u - g$, $g - r$, $r - i$ and $i - z$ colors of the thin and thick disk stars were computed at each spectral subtype, as shown in Figure 11. There are no significant color differences between the thin and thick disks at a given spectral type. This further suggests that the SLoMaSS stars are not probing a large spread in metallicity.

4.3.3. Chromospheric Activity

Finally, if the thick disk is an older system (as suggested by its hotter kinematics), it should possess a lower fraction of active stars (West et al. 2004, 2006). The chromospheric activity timescale varies with mass, such that higher mass stars lose their activity sooner (after ~ 1 Gyr) than their low-mass counterparts (~ 10 Gyr). To observationally quantify chromospheric activity, the H α equivalent width (EW) is measured for each M dwarf. We employed the technique introduced in West et al. (2004) and described in Bochanski et al. (2007), selecting chromospherically active and inactive stars at each spectral type. To be classified as active, a star must have an EW of 1 \AA , and pass additional signal-to-noise and error tests described in West et al. (2004). Figure 12 shows the active fraction of stars as a function of spectral type for both disk populations. While most early-type M dwarfs (M0-M3) lose their activity quite rapidly, the later types (M5) possess smaller active fractions in the thick disk, and exhibit the expected behavior of older systems. However, these results are only suggestive, as populations older than ~ 4 Gyr require M dwarfs with types later than M5 in order to be effective probes of the age (West et al. 2007).

5. CONCLUSIONS

The Milky Way (along with other spiral galaxies) is evidently a composite of a few major smooth components (the thin and thick disks and the halo) and many smaller structures, such as the tidal debris streams from the Sagittarius dwarf galaxy. Using spectra, proper motions and photometry along one Galactic sight-line, we studied the kinematic and structural distributions of the smooth thin and thick disks as a function of vertical distance from the Plane. We fit two-component Gaussians

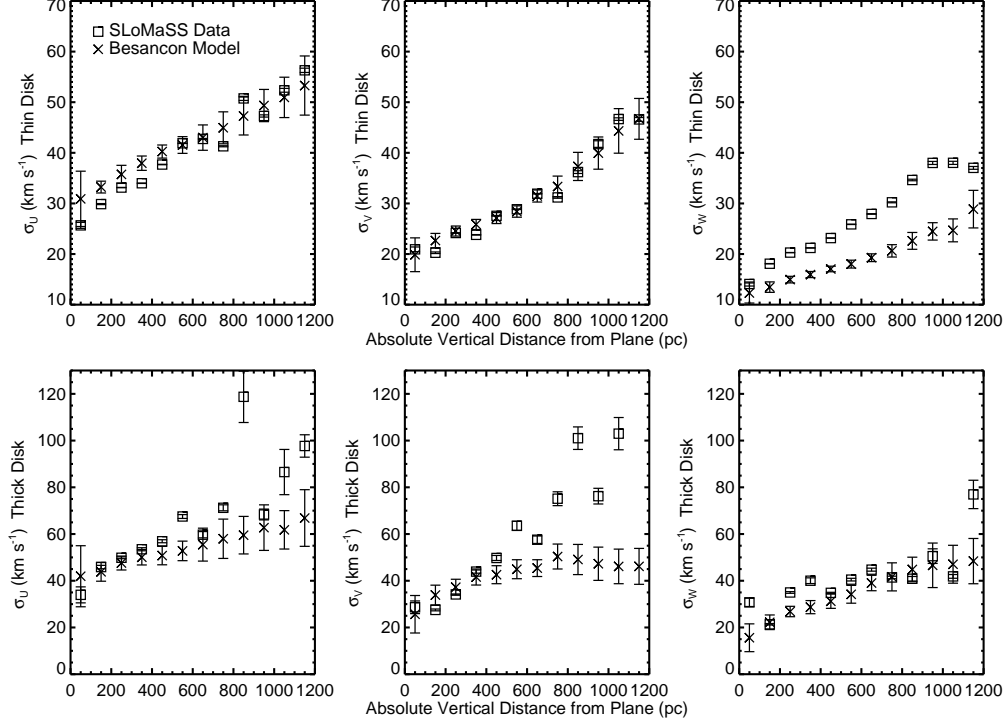


FIG. 8.— Thin Disk (upper panels) and Thick Disk (lower panels) velocity dispersions for SLoMaSS data (open squares) and Besançon model predictions (crosses). The model reproduces general trends, such as increased dispersion with distance from the Galactic Plane. The thin disk W velocity dispersions are systematically low, as are the thick disk V dispersions at large heights. This is probably due to the assumed age-velocity dispersion relation, as explained in §4.2.4.

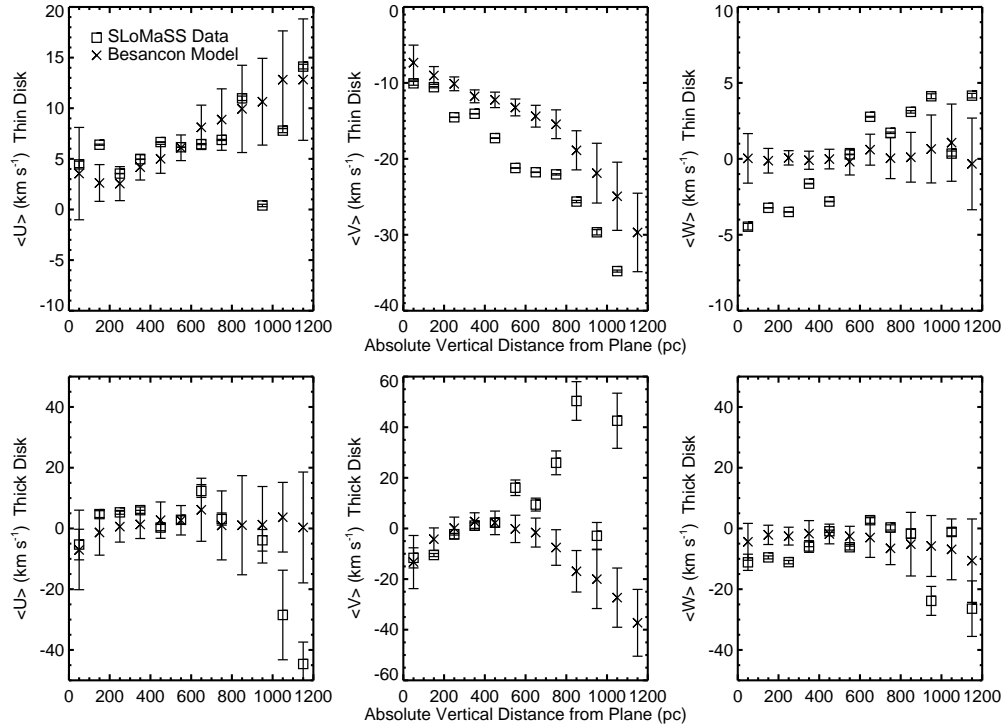


FIG. 9.— Thin Disk (upper panels) and Thick Disk (lower panels) mean velocities for SLoMaSS data (open squares) and Besançon model predictions (crosses). The thin disk mean V velocities predicted by the Besançon models are systematically low, while the observed thick disk mean V velocities diverge at large Galactic heights.

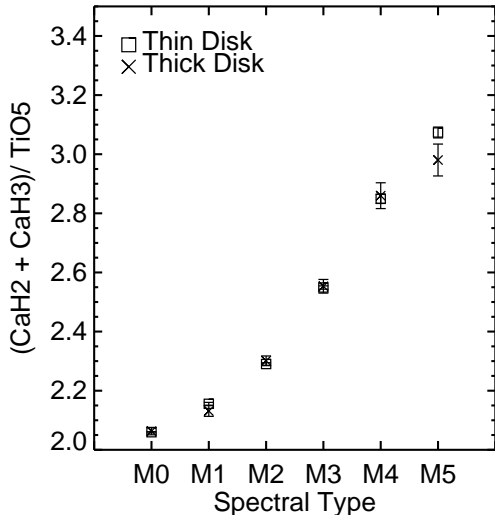


FIG. 10.— The metallicity-sensitive ratio of $(\text{CaH2} + \text{CaH3}) / \text{TiO5}$ vs. Spectral Type for the thin (open squares) and thick (crosses) disk populations. Higher ratio values indicate a higher metallicity (Burgasser & Kirkpatrick 2006). Within the error bars, the thin and thick disk populations exhibit very similar behavior, indicating that the sample may not be probing a large spread ($\gtrsim 1$ dex) in metallicity.

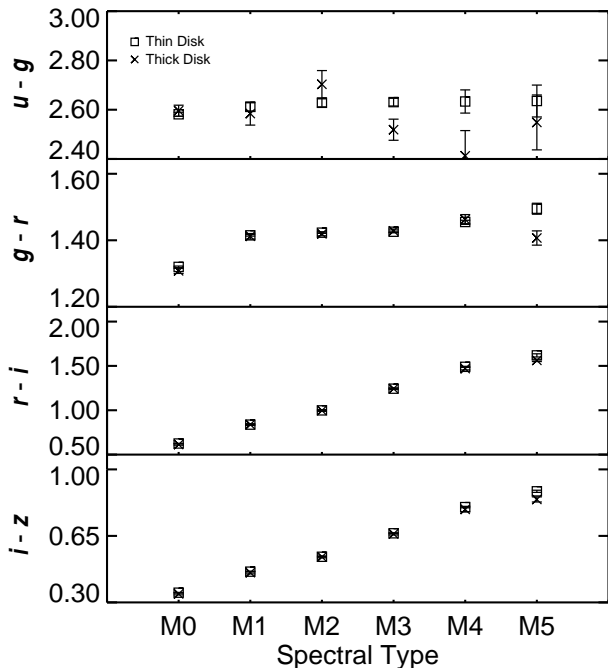


FIG. 11.— The *ugriz* colors as a function of spectral type for the thin (open squares) and thick (crosses) disk populations. The colors of both populations agree within the errors, suggesting that the M dwarfs in SLoMaSS do not cover a large metallicity range.

to the *UVW* distributions as a function of height, placing new constraints on the thin and thick disk velocity dispersions.

This sample was then employed to test the predictions of current Galactic models. The Besançon model was chosen for comparison, since it is widely accepted as a standard and models the kinematics of stellar populations. We generated a suite of 25 models, and each model was sampled to be consistent with the colors and distance

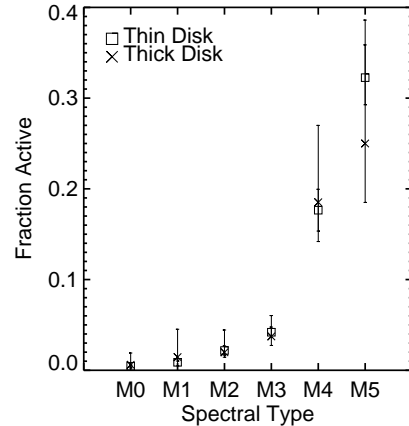


FIG. 12.— Shown is active fraction of stars as a function of spectral type for the thin (open squares) and thick (crosses) disk populations. An older population would show a lower active fraction, as suggested by the thick disk stars in the M5 bin.

distribution of SLoMaSS. The bulk kinematic properties of the data and model were compared. They agree to $\sim 10 \text{ km s}^{-1}$, placing a limit on the accuracy of model predictions. However, σ_W is poorly fit by the model, suggesting that further investigation into modeling the kinematics of the thin and thick disks is necessary. In particular, the age-velocity dispersion plays an important role in the kinematic predictions, and a more exact definition of this relation is required.

SLoMaSS was divided kinematically, assigning membership of each star to either the thin or thick disk. We inspected the two populations as functions of spectral type, searching for observable differences in the metallicity, colors and chromospheric activity. While there was little observed difference between the metallicity and color distributions, the activity fraction distribution suggests that the thick disk displays an activity level consistent with an older population, although this result is purely suggestive and needs to be re-examined with later spectral types. The lack of a strong observable signal may have several causes. Primarily, kinematic separation of populations is not perfect, as stars with extreme kinematics in one population (i.e. the thin disk) can masquerade as members of the other population. This would dilute observable differences, and in our case, the more numerous thin disk population may be polluting the thick disk sample, despite our best efforts to minimize this effect. Secondly, the intrinsic properties (i.e. metallicity) of the stars that compose the thin and thick disks are drawn from overlapping distributions. Stars that are at the edges of these distributions would also blur the distinction among observable properties, clouding the best efforts of the observer. Further investigations using stellar tracers along the entire main sequence should alleviate some of these issues.

The authors would like to thank Neil Reid, whose comments greatly improved the scope of the analysis. We also wish to thank Lucianne Walkowicz and Hugh Harris for their early work on this project. We also gratefully acknowledge the support of NSF grants AST02-05875 and AST06-07644 and NASA ADP grant NAG5-13111.

Funding for the SDSS and SDSS-II has been provided by the Alfred P. Sloan Foundation, the Partic-

icipating Institutions, the National Science Foundation, the U.S. Department of Energy, the National Aeronautics and Space Administration, the Japanese Monbukagakusho, the Max Planck Society, and the Higher Education Funding Council for England. The SDSS Web Site is <http://www.sdss.org/>.

The SDSS is managed by the Astrophysical Research Consortium for the Participating Institutions. The Participating Institutions are the American Museum of Natural History, Astrophysical Institute Potsdam, University of Basel, University of Cambridge, Case Western Reserve University, University of Chicago, Drexel Uni-

versity, Fermilab, the Institute for Advanced Study, the Japan Participation Group, Johns Hopkins University, the Joint Institute for Nuclear Astrophysics, the Kavli Institute for Particle Astrophysics and Cosmology, the Korean Scientist Group, the Chinese Academy of Sciences (LAMOST), Los Alamos National Laboratory, the Max-Planck-Institute for Astronomy (MPIA), the Max-Planck-Institute for Astrophysics (MPA), New Mexico State University, Ohio State University, University of Pittsburgh, University of Portsmouth, Princeton University, the United States Naval Observatory, and the University of Washington.

REFERENCES

- Abazajian, K., et al. 2004, *AJ*, 128, 502
 Adelman-McCarthy, J. K., et al. 2006, *ApJS*, 162, 38
 —. 2007
 Bahcall, J. N., & Soneira, R. M. 1980, *ApJS*, 44, 73
 Belokurov, V., et al. 2006, *ApJ*, 642, L137
 Bensby, T., Feltzing, S., & Lundström, I. 2003, *A&A*, 410, 527
 Bienayme, O., Robin, A. C., & Creze, M. 1987, *A&A*, 180, 94
 Binney, J., Gerhard, O., & Spergel, D. 1997, *MNRAS*, 288, 365
 Bochanski, J. J., Hawley, S. L., Reid, I. N., Covey, K. R., West, A. A., Tinney, C. G., & Gizis, J. E. 2005, *AJ*, 130, 1871
 Bochanski, J. J., West, A. A., Hawley, S. L., & Covey, K. R. 2007, *AJ*, 133, 531
 Brook, C. B., Kawata, D., Gibson, B. K., & Freeman, K. C. 2004, *ApJ*, 612, 894
 Burgasser, A. J., & Kirkpatrick, J. D. 2006, *ApJ*, 645, 1485
 Buser, R., Rong, J., & Karaali, S. 1999, *A&A*, 348, 98
 Chen, B., et al. 2001, *ApJ*, 553, 184
 Chiba, M., & Beers, T. C. 2000, *AJ*, 119, 2843
 Cohen, M. 1995, *ApJ*, 444, 874
 Covey, K. C., et al. 2007a, *AJ*, in preparation
 —. 2007b, *AJ*, in preparation
 Creze, M., Chereul, E., Bienayme, O., & Pichon, C. 1998, *A&A*, 329, 920
 Dalcanton, J. J., Spergel, D. N., & Summers, F. J. 1997, *ApJ*, 482, 659
 Davenport, J. R. A., West, A. A., Matthiesen, C. K., Schmieding, M., & Kobelski, A. 2006, *PASP*, 118, 1679
 Dehnen, W., & Binney, J. J. 1998, *MNRAS*, 298, 387
 Delhaye, J. 1965, in *Galactic Structure*, ed. A. Blaauw & M. Schmidt, 61–
 Eisenstein, D. J., et al. 2001, *AJ*, 122, 2267
 Feltzing, S., Bensby, T., & Lundström, I. 2003, *A&A*, 397, L1
 Frieman, J. A., et al. 2007, *AJ*, submitted
 Fuhrmann, K. 1998, *A&A*, 338, 161
 Fukugita, M., Ichikawa, T., Gunn, J. E., Doi, M., Shimasaku, K., & Schneider, D. P. 1996, *AJ*, 111, 1748
 Giclas, H. L., Burnham, R., & Thomas, N. G. 1971, *Lowell proper motion survey Northern Hemisphere. The G numbered stars. 8991 stars fainter than magnitude 8 with motions < 0".26/year (Flagstaff, Arizona: Lowell Observatory, 1971)*
 Gilmore, G., & Reid, N. 1983, *MNRAS*, 202, 1025
 Gizis, J. E. 1997, *AJ*, 113, 806
 Gizis, J. E., Reid, I. N., & Hawley, S. L. 2002, *AJ*, 123, 3356
 Gliese, W., & Jahreiss, H. 1991, *Preliminary Version of the Third Catalogue of Nearby Stars*, Tech. rep.
 Gomez, A. E., Grenier, S., Udry, S., Haywood, M., Meillon, L., Sabas, V., Sellier, A., & Morin, D. 1997, in *ESA SP-402: Hipparcos - Venice '97*, 621–624
 Governato, F., Willman, B., Mayer, L., Brooks, A., Stinson, G., Valenzuela, O., Wadsley, J., & Quinn, T. 2007, *MNRAS*, 374, 1479
 Gunn, J. E., et al. 1998, *AJ*, 116, 3040
 —. 2006, *AJ*, 131, 2332
 Hawley, S. L., Gizis, J. E., & Reid, I. N. 1996, *AJ*, 112, 2799
 Hawley, S. L., et al. 2002, *AJ*, 123, 3409
 Hogg, D. W., Finkbeiner, D. P., Schlegel, D. J., & Gunn, J. E. 2001, *AJ*, 122, 2129
 Ibata, R. A., Gilmore, G., & Irwin, M. J. 1994, *Nature*, 370, 194
 Ivezić, Z., Allyn Smith, J., Miknaitis, G., Lin, H., & Tucker, D. 2007, *ArXiv Astrophysics e-prints*
 Ivezić, Ž., et al. 2003, *Memorie della Societa Astronomica Italiana*, 74, 978
 —. 2004, *Astronomische Nachrichten*, 325, 583
 Johnson, D. R. H., & Soderblom, D. R. 1987, *AJ*, 93, 864
 Juric, M., et al. 2005, *ArXiv Astrophysics e-prints*
 Kerber, L. O., Javiel, S. C., & Santiago, B. X. 2001, *A&A*, 365, 424
 Kilic, M. et al. 2006, *AJ*, 131, 582
 Larsen, J. A., & Humphreys, R. M. 2003, *AJ*, 125, 1958
 Laughlin, G., Bodenheimer, P., & Adams, F. C. 1997, *ApJ*, 482, 420
 Lejeune, T., Cuisinier, F., & Buser, R. 1998, *A&AS*, 130, 65
 Lépine, S., Rich, R. M., & Shara, M. M. 2003, *AJ*, 125, 1598
 Lutz, T. E., & Uppgren, A. R. 1980, *AJ*, 85, 1390
 Luyten, W. J. 1979, *LHS catalogue. A catalogue of stars with proper motions exceeding 0".5 annually (Minneapolis: University of Minnesota, 1979, 2nd ed.)*
 Majewski, S. R. 1993, *ARA&A*, 31, 575
 Martini, P., & Osmer, P. S. 1998, *AJ*, 116, 2513
 Mendez, R. A., & van Altena, W. F. 1996, *AJ*, 112, 655
 Munn, J. A., et al. 2004, *AJ*, 127, 3034
 Newberg, H. J., et al. 2002, *ApJ*, 569, 245
 Ng, Y. K., Bertelli, G., Chiosi, C., & Bressan, A. 1997, *A&A*, 324, 65
 Norris, J. E. 1999, *Ap&SS*, 265, 213
 Ojha, D. K., Bienaymé, O., Mohan, V., & Robin, A. C. 1999, *A&A*, 351, 945
 Ojha, D. K., Bienaymé, O., Robin, A. C., Creze, M., & Mohan, V. 1996, *A&A*, 311, 456
 Phleps, S., Meisenheimer, K., Fuchs, B., & Wolf, C. 2000, *A&A*, 356, 108
 Pier, J. R., Munn, J. A., Hindsley, R. B., Hennessy, G. S., Kent, S. M., Lupton, R. H., & Ivezić, Z. 2003, *AJ*, 125, 1559
 Ratnatunga, K. U., & Uppgren, A. R. 1997, *ApJ*, 476, 811
 Raymond, S. N., et al. 2003, *AJ*, 125, 2621
 Reid, I. N., Gizis, J. E., Cohen, J. G., Pahre, M. A., Hogg, D. W., Cowie, L., Hu, E., & Songaila, A. 1997, *PASP*, 109, 559
 Reid, I. N., Gizis, J. E., & Hawley, S. L. 2002, *AJ*, 124, 2721
 Reid, I. N., Hawley, S. L., & Gizis, J. E. 1995, *AJ*, 110, 1838
 Reid, N. 1993, in *ASP Conf. Ser. 49: Galaxy Evolution. The Milky Way Perspective*, ed. S. R. Majewski, 37–
 Reid, N., & Majewski, S. R. 1993, *ApJ*, 409, 635
 Richards, G. T., et al. 2002, *AJ*, 123, 2945
 Robin, A. C., Reylé, C., Derrière, S., & Picaud, S. 2003, *A&A*, 409, 523
 Rocha-Pinto, H. J., Flynn, C., Scalo, J., Hänninen, J., Maciel, W. J., & Hensler, G. 2004, *A&A*, 423, 517
 Sako, M., et al. 2005, *ArXiv Astrophysics e-prints*
 Schlegel, D. J., Finkbeiner, D. P., & Davis, M. 1998, *ApJ*, 500, 525
 Schmidt, S. J., Cruz, K. L., Bongiorno, B. J., Liebert, J., & Reid, I. N. 2007, *AJ*, 133, 2258
 Sesar, B., et al. 2007, *ArXiv e-prints*, 704
 Siegel, M. H., Majewski, S. R., Reid, I. N., & Thompson, I. B. 2002, *ApJ*, 578, 151
 Silvestri, N. M., et al. 2006, *AJ*, 131, 1674
 Smith, J. A., et al. 2002, *AJ*, 123, 2121
 Smolčić, V. et al. 2004, *ApJ*, 615, L141
 Stoughton, C., et al. 2002, *AJ*, 123, 485
 Strauss, M. A., et al. 2002, *AJ*, 124, 1810
 Tonry, J., & Davis, M. 1979, *AJ*, 84, 1511
 Tucker, D. L. et al. 2006, *Astronomische Nachrichten*, 327, 821

- Vallenari, A., Pasetto, S., Bertelli, G., Chiosi, C., Spagna, A., & Lattanzi, M. 2006, *A&A*, 451, 125
- Vanden Berk, D. E. et al. 2005, *AJ*, 129, 2047
- Vysotsky, A. N. 1956, *AJ*, 61, 201
- Walkowicz, L. M., Hawley, S. L., & West, A. A. 2004, *PASP*, 116, 1105
- Weis, E. W., & Uggren, A. R. 1995, *AJ*, 109, 812
- West, A. A., Bochanski, J. J., Hawley, S. L., Cruz, K. L., Covey, K. R., Silvestri, N. M., Reid, I. N., & Liebert, J. 2006, *AJ*, 132, 2507
- West, A. A., Walkowicz, L. M., & Hawley, S. L. 2005, *PASP*, 117, 706
- West, A. A., et al. 2004, *AJ*, 128, 426
- . 2007, *AJ*, in preparation
- Wielen, R. 1977, *A&A*, 60, 263
- Wilson, O., & Woolley, R. 1970, *MNRAS*, 148, 463
- Wolf, V. M., & Wallerstein, G. 2006, *PASP*, 118, 218
- Yanny, B. et al. 2003, *ApJ*, 588, 824
- Yanny, B., et al. 2000, *ApJ*, 540, 825
- Yoachim, P., & Dalcanton, J. J. 2006, *AJ*, 131, 226
- York, D. G., et al. 2000, *AJ*, 120, 1579